Performance comparison of optimum power flow based on the sequential second-order cone programming in unbalanced low voltage distribution networks with distributed generators

Dilan I. Manamperi[1], Janaka B. Ekanayake[2, 3]

[1] Ceylon Electricity Board, Sri Lanka.

[2] Department of Electrical and Electronic Engineering, University of Peradeniya, Peradeniya, Sri Lanka.

[3] School of Engineering, Cardiff University, UK

Correspondence

Dilan I. Manamperi, Ceylon Electricity Board, Sri Lanka

Email: indoopa2010@gmail.com

Data availability statement

The data that support the findings of this study are available from the corresponding author upon reasonable request.

Summary: A solution technique using sequential sequential second-order cone programming to solve the optimum power flow problem in low voltage (LV) distribution networks with distributed generation is developed. A novel bound tightening method is suggested to get exact solutions with few iterations. A novel approximation method is suggested to increase exactness by approximating phase angle dependant components. The performance of the suggested solution method is compared with linear programming, semidefinite programming, genetic algorithm, particle swarm, sequential quadratic programming with multiple start points, and global search-based optimization methods. The exactness of the generated solutions is validated after comparison with a load flow. The proposed algorithm provides better performance in optimality, execution time, and exactness compared to other methods.

KEYWORKS: Optimum power flow, power distribution system, distributed generation, second-order cone programming

List of Symbols and Abbreviations:

$\boldsymbol{U_{A_m}}$, Complex voltage at node m of phase A; $\boldsymbol{I_{A_{mn}}}$, Complex current of phase A of line m-n; $p_{A_{mn}}$, Active powers flowing from node m to n in phase A; $q_{A_{mn}}$, Reactive powers flowing from node m to n in phase A; $\mathrm{P}_{\mathrm{A_n}}^{\mathrm{C}}$, Real power consumption at phase A of node n; $\mathrm{Q}_{\mathrm{A_n}}^{\mathrm{C}}$, Reactive power consumption at phase A of node n; $\mathrm{P}_{\mathrm{A_n}}^{\mathrm{G}}$, Real power generation from the PV inverters at phase A of node n; $Q_{A_n}^{G}$, Reactive power generation from the PV inverters at phase A of node n; $P_A^{Cur}{}_n$, Real power curtailment from the PV inverters at phase A of node n; $I_A^R{}_m$, Real part of $\boldsymbol{I_{A_{mn}}}$; $I_A^{Im}{}_m$, Imaginary part of $\boldsymbol{I_{A_{mn}}}$; $U_A^R{}_m$, Real part of $\boldsymbol{U_{A_m}}$; $\mathrm{U}_{\mathrm{A}}^{\mathrm{Im}}{}_{\mathrm{m}}$, Imaginary part of $\boldsymbol{U_{A_m}}$; W_{A_m}, Squared magnitude of $\boldsymbol{U_{A_m}}$; $L_{A_{mn}}$, Squared magnitude of $\boldsymbol{I_{A_{mn}}}$; LVDN, Low Voltage Distribution Networks; DG, distributed generation; PV, Photovoltaic; OLTC, On Load Tap Changing; OPF, Optimum Power Flow; SOCP, Second Order Cone Programming

1. INTRODUCTION

Optimum power flow (OPF) is used as a tool to optimally control controllable devices such as smart inverters, batteries, tap changing transformers, and static var compensators in LV networks. OPF for transmission networks is widely discussed in the literature, and they are used in day-to-day operations in transmission system control centres.[1,2] With the increased penetration of renewable energy in low voltage distribution systems, the use of OPF for controlling power flows in distribution systems is considered. There are several techniques to solve the optimum power flow problem in distribution systems.

Some researchers use evolutionary computation techniques like genetic algorithms and particle swarm optimization in their centralized control schemes. Grey wolf optimizer is used by Mahmoud et al[3] to prevent voltage violation in medium voltage distribution systems by minimizing PV power curtailments and tap movement rate. A genetic algorithm-based method is used by Senjyu et al[4]

for the centralized cooperation control of sending voltage, and static voltage regulators (SVR), shunt capacitor (SC), and static var compensators (SVC). Evolutionary computation techniques could be time-consuming because of the extensive solution space available with different controllable devices.

Local optimization methods are used to obtain a local solution to OPF. The predictor-corrector interior-point algorithm is used by Nguyen et al[5] to obtain exact local solutions to OPF for an unbalanced MV distribution system with high PV penetration. There is a tendency of converging to the local optimum closer to the start point in local optimization methods.

Considering the slow convergence and local optimality of the OPF techniques discussed above, the convex optimization techniques for solving OPF are introduced. This technique is widely used in 3 phase unbalanced OPF.[6,7] Since the OPF problem is non-convex, convex relaxations or approximations are used in these studies to make the OPF problem convex. Linear programming (LP), second-order cone programming (SOCP), and semidefinite programming (SDP) are widely used convex optimization techniques for solving OPF.

A linear program is used by Richardson et al[8] to determine the optimal charging rate of electric vehicles connected to the LV distribution system. Voltage sensitivity to real power is used to linearize the power flow equations. A residential energy consumption scheduling algorithm for areas with high penetration of rooftop PV units is proposed by Yao et al.[9] Equations with voltage sensitivities to the active and reactive powers are used instead of load flow equations. OPF for an unbalanced three-phase distribution network is represented as a convex quadratic program in Robbins et al.[10] Due to the nonlinear nature of power flow equations, linearization assumptions considered in the above studies can generate inaccurate solutions.

Semidefinite programming (SDP) model to minimize power loss and generation cost in unbalanced distribution systems is proposed by Dall'Anese et al[6] based on the bus injection model (BIM). SDP model to minimize generation cost is proposed by Gan et al[11] based on bus injection model (BIM) and branch flow model (BFM). However, obtaining exact solutions is impossible for some practical three-phase distribution systems due to the assumptions considered in relaxations and approximations.[12,13] According to Louca et al,[12] in practice, many instances of OPF yield semidefinite relaxations with optimal solutions of high rank, which are not exact. Limits of the SDP approach are highlighted by Lesieutre et al[13] by providing transmission system test cases that

fail to give a physically meaningful solution with a non-zero duality gap. To improve semidefinite relaxation, a rank minimization algorithm is suggested by Louca et al.[12] The objective function is modified using a heuristic method to extract rank-1 solutions from low-rank solutions by Somayeh et al.[14] The above methods represent OPF as an SDP and computing time of SDP increases rapidly with the number of variables compared to the second-order cone programming (SOCP) approach.[15,16,17,18] Also, SDP solvers are still not numerically robust.[7]

Global optimization techniques which rely on the iterative use of convex optimization are used to obtain the global optimality of OPF. Sequential quadratic programming (SQP) is used by Su et al[19] to solve OPF in unbalanced four-wire distribution systems for improving voltage profile while minimizing line losses and generation costs. A branch and bound-based global optimization method is suggested by Gopalakrishnan et al[20] to solve OPF in unbalanced distribution systems. Despite having the global optimum, branch and bound based methods are time-consuming.[21]

Second-order cone programming (SOCP) is widely used to solve the balanced 3 phase OPF.[22,15] SOCP is used by Farivar[22] for optimum inverter VAR control in balanced three-phase distribution systems. SOCP is used to solve the OPF problem to determine the optimal dispatch of deterministic inverter-interfaced energy storage in an unbalanced distribution feeder with significant solar PV penetration by Nazir et al.[7] The solution of the SOCP is used to initialize a nonlinear program (NLP) to ensure a physically realizable solution. SOCP relaxation also provides infeasible solutions to OPF in some conditions.[23,24] Proofs are provided by Low[24] for balanced SOCP OPF relaxation to be exact when both constraints on real and reactive power injections are not binding at both ends of a line, upper bounds on voltage magnitudes are not binding, and voltage angles across each line are sufficiently close. However, these conditions cannot be satisfied in many practical networks. Increasingly tightening cutting planes are used in [15,25] to extract physically meaningful solutions to balanced OPF after applying second-order cone (SOC) relaxation. A higher computation time taken for several iterations can be considered as a drawback in these methods. A heuristic method is suggested by Yuan et al[16] to extract feasible solutions from relaxed solutions. SOCP is used in[26] to provide a warm start to solve the OPF in unbalanced distribution systems using a non-linear program (NLP). Solving NLP is time-consuming for larger networks.

In this paper, a sequential SOCP methodology is suggested by modifying the rectangular voltage-current formulation of a three-phase branch flow model with approximations and relaxations, thus making the problem convex. The proposed methodology enables to achieve exact solutions by gradually limiting the solutions space to load flow solutions and solving load flow, including the previous SOCP outputs. Currents from load flow with gradually decreasing constants are used as cutting planes for second-order cone relaxations. Sufficiently exact solutions are obtained under ten iterations of the optimization program resulting in lesser computation time.

The performance of the proposed algorithm is compared with the methods suggested in[10,11,19] global search, particle swarm, and genetic algorithms.

The contributions of the paper are:

1. A sequential SOCP based optimization-based technique is introduced for obtaining accurate solutions for OPF problems in unbalanced low and medium voltage distribution systems with voltage rise above permissible limits.

   As discussed in the literature, solutions obtained from convex relaxations are not exact for practical unbalance distribution systems. Sequential convex optimization techniques are introduced in the litreture[15,25] to address this issue in balanced three-phase systems. The Sequential SOCP technique proposed in this paper is designed to use in unbalanced distribution networks.

   Constraints on phase angle difference are missing on many unbalanced OPF solving methods.[27] Requirement for a bound on voltage angles is mitigated due to the use of novel approximation technique to approximate angle-dependent components in power flow equations. Due to that sufficiently exact solutions are provided for both low ($R/X<1$) and medium voltage networks ($R/X>1$). Heuristic optimisation methods are used in previous studies to control voltage in distribution grids with DG.[28,29] For the first time to our knowledge faster convex optimization based OPF solving method is tested for unbalanced distribution systems with voltage rise above permissible limits (PV penetration greater than 500%) in this paper.

2. Faster execution time due to fewer iterations of SOCP

   The operational cost of distribution systems is significantly lower than transmission systems. Also with high solar penetration and varying consumption, operational status should be determined dynamically. Therefore achieving a feasible operating point quickly is more important than obtaining global optimum. SOC relaxation is tightened gradually using outputs from load-flow. SOC tightening constraints is simpler, and the computational burden is low in the proposed method compared to other cutting plane methods.

3. Seven optimization techniques are used to solve the same OPF problem, and their performances are compared.

   Outputs of many convex optimization methods differ depending on loads and network conditions. Infeasibility is reported for some time instances when simulated over a time frame.[30] Recently, several convex optimization techniques are tested for two balanced networks in [30]. Several heuristic optimization techniques are compared in [31] without PV generation. For the first time to our knowledge, different optimization techniques are compared for a wide range of unbalanced networks with high PV penetration in this paper.

   Compared to convex optimization-based OPF solving methods, the suggested algorithm provides accurate (exact) solutions. As observed in the case studies, the inaccuracies of methods suggested in the previous literature increase with the size of the distribution network and the reverse power flow.

   Compared to heuristic (genetic and particle swarm) and global optimization methods, the execution time of the proposed algorithm is considerably shorter. The optimality of the proposed algorithm is close to the global optimum for some simulated test cases. Simulation of heuristic optimizations and global optimization provides the ability to compare the simulation results of convex optimization methods with possible global optimums. Optimum setpoints are generated randomly in heuristic optimization methods. Therefore, there is a chance to obtain global optimum or more optimum setpoints using heuristic optimization methods.

2. METHODOLOGY

2.1 Representative equations for the optimization problem

Kron reduction technique was used to reduce the four-wire distribution system to a three-wire system.[28] It was assumed that neutral was grounded at multiple points. The radial power flow equations were represented by DistFlow equations.[29]

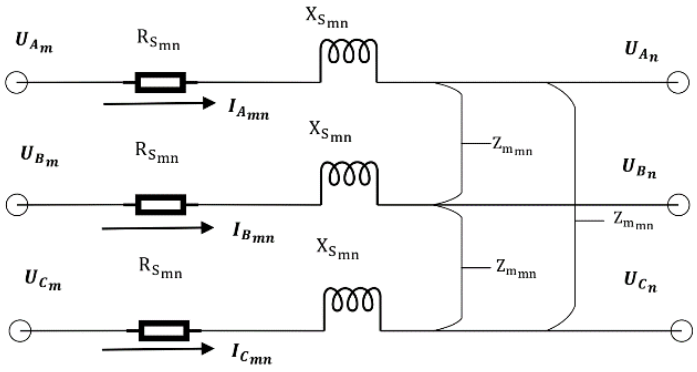

Figure 1 - Diagram of m-n line segment

For the m-n line segment shown in Figure 1, from the power balance of the three-phase lines, equation (1) was derived.[10,19] Power flown to node m equals the summation of power flown out of node n, line loss, and power generation/consumption at node n.

$$\begin{bmatrix} \boldsymbol{S_{A_{mn}}} \\ \boldsymbol{S_{B_{mn}}} \\ \boldsymbol{S_{C_{mn}}} \end{bmatrix} = \sum_{k:(j,k)\in E} \begin{bmatrix} \boldsymbol{S_{A_{nk}}} \\ \boldsymbol{S_{B_{nk}}} \\ \boldsymbol{S_{C_{nk}}} \end{bmatrix} + diag\left(\begin{bmatrix} Z_{\mathrm{s_{mn}}} & Z_{\mathrm{m_{mn}}} & Z_{\mathrm{m_{mn}}} \\ Z_{\mathrm{m_{mn}}} & Z_{\mathrm{s_{mn}}} & Z_{\mathrm{m_{mn}}} \\ Z_{\mathrm{m_{mn}}} & Z_{\mathrm{m_{mn}}} & Z_{\mathrm{s_{mn}}} \end{bmatrix} \begin{bmatrix} \boldsymbol{I_{A_{mn}}} \\ \boldsymbol{I_{B_{mn}}} \\ \boldsymbol{I_{C_{mn}}} \end{bmatrix} \begin{bmatrix} \boldsymbol{I_{A_{mn}}} \\ \boldsymbol{I_{B_{mn}}} \\ \boldsymbol{I_{C_{mn}}} \end{bmatrix}^{H} \right) + \begin{bmatrix} \boldsymbol{S_{A_n}} \\ \boldsymbol{S_{B_n}} \\ \boldsymbol{S_{C_n}} \end{bmatrix} \quad (1)$$

where,

$\boldsymbol{S_{A_{mn}}} = p_{A_{mn}} + jq_{A_{mn}}$

$\boldsymbol{S_{A_n}} = \mathrm{P_{A_n}^C} - \mathrm{P_{A_n}^G} + {P_A^{Cur}}_n + \mathrm{j}(\mathrm{Q_{A_n}^C} \pm Q_{A_n}^G)$

H denotes the Hermitian transpose.

The power flow equations of phases A, B, and C were obtained from expanding the first, second, and third rows. By considering the real parts of the first row to represent the active power flow of phase A, equation (2) was obtained.

$$p_{A_{mn}} = \sum_{k:(j,k)\in E} p_{A_{nk}} + \mathrm{P_{A_n}^C} - \mathrm{P_{A_n}^G} + {P_A^{Cur}}_n + \mathrm{Re}\{\boldsymbol{I_{A_{mn}}}^* \times (\mathrm{R_{s_{mn}}} \boldsymbol{I_{A_{mn}}} + \mathrm{R_{m_{mn}}} \boldsymbol{I_{B_{mn}}} + \mathrm{R_{m_{mn}}} \boldsymbol{I_{C_{mn}}})\} \quad (2)$$

By considering the imaginary parts of the first row to represent phase A's reactive power flow, equation (3) was obtained.

$$q_{A_{mn}} = \sum_{k:(j,k)\in E} q_{A_{nk}} + \mathrm{Q}_{\mathrm{A_n}}^{\mathrm{C}} \pm Q_{A_n}^{G} + \mathrm{Im}\left\{\boldsymbol{I_{A_{mn}}}^{*} \times \left(\mathrm{R}_{\mathrm{s_{mn}}}\boldsymbol{I_{A_{mn}}} + \mathrm{R}_{\mathrm{m_{mn}}}\boldsymbol{I_{B_{mn}}} + \mathrm{R}_{\mathrm{m_{mn}}}\boldsymbol{I_{C_{mn}}}\right)\right\} \quad (3)$$

where,

$\boldsymbol{I_{A_{mn}}}$, $p_{A_{mn}}$, $q_{A_{mn}}$ are the complex current, active and reactive powers flowing from node m to n in phase A.

$\mathrm{P}_{\mathrm{A_n}}^{\mathrm{C}}$ and $\mathrm{Q}_{\mathrm{A_n}}^{\mathrm{C}}$ are the real and reactive power consumption of phase A of node n.

$\mathrm{P}_{\mathrm{A_n}}^{\mathrm{G}}$, $Q_{A_n}^{G}$ and $P_A^{Cur}{}_n$ are the real and reactive power generation and active power curtailment from the PVs and inverters in phase A of node n.

Two new variables, $W_{A_m} = |\boldsymbol{U_{A_m}}|^2$ and $L_{A_{mn}} = |\boldsymbol{I_{A_{mn}}}|^2$, for every bus and every line were introduced. Then variables in non-convex terms ($U_A^R{}_n, I_A^R{}_{mn}, U_A^{Im}{}_n, I_A^{Im}{}_{mn}$) of equations (1) and (2) were replaced by values obtained from load flow. The exact equations used are given in Appendix A as equations A1 and A2.

Equations for apparent power flow at node m to n were derived from Equation (4).[19]

$$\begin{bmatrix} \boldsymbol{S_{A_{mn}}} \\ \boldsymbol{S_{B_{mn}}} \\ \boldsymbol{S_{C_{mn}}} \end{bmatrix} = diag\left(\begin{bmatrix} \boldsymbol{U_{A_m}} \\ \boldsymbol{U_{B_m}} \\ \boldsymbol{U_{C_m}} \end{bmatrix}\begin{bmatrix} \boldsymbol{I_{A_{mn}}} \\ \boldsymbol{I_{B_{mn}}} \\ \boldsymbol{I_{C_{mn}}} \end{bmatrix}^{H}\right) \quad (4)$$

By expanding the first row,

$$\boldsymbol{S_{A_{mn}}} = \boldsymbol{U_{A_m}}\boldsymbol{I_{A_{mn}}}^{*} \quad (5)$$

where $\boldsymbol{U_{A_m}}$ and $\boldsymbol{U_{A_n}}$ are the complex voltage at node m and n of phase A and are given by $\boldsymbol{U_{A_m}} = U_A^R{}_m + jU_A^{Im}{}_m$ and $\boldsymbol{U_{A_n}} = U_A^R{}_n + jU_A^{Im}{}_n$

Similarly, current flown from m to n of phase A, $\boldsymbol{I_{A_{mn}}} = I_A^R{}_m + jI_A^{Im}{}_m$

After the multiplication of both sides of (5) by $\boldsymbol{S_{A_{mn}}}^{*}$,

$$\boldsymbol{S_{A_{mn}}} \times \boldsymbol{S_{A_{mn}}}^{*} = \boldsymbol{U_{A_m}}\boldsymbol{I_{A_{mn}}}^{*} \times \boldsymbol{S_{A_{mn}}}^{*}$$

$$\boldsymbol{S_{A_{mn}}} \times \boldsymbol{S_{A_{mn}}}^{*} = \boldsymbol{U_{A_m}}\boldsymbol{I_{A_{mn}}}^{*} \times \boldsymbol{U_{A_m}}^{*}\boldsymbol{I_{A_{mn}}}$$

$$(p_{A_{mn}} + jq_{A_{mn}}) \times (p_{A_{mn}} + jq_{A_{mn}})^* = \boldsymbol{U_{A_m} U_{A_m}}^* \times \boldsymbol{I_{A_{mn}}}^* \boldsymbol{I_{A_{mn}}}$$

After simplifying the above equation, equation (6) was obtained.

$$p_{A_{mn}}^2 + q_{A_{mn}}^2 = \left|\boldsymbol{U_{A_m}}\right|^2 \left|\boldsymbol{I_{A_{mn}}}\right|^2 \quad (6)$$

Then with substitutions, equation (6) was rewritten as:

$$\boldsymbol{W_{A_{mn}} L_{A_m}} = p_{A_{mn}}^2 + q_{A_{mn}}^2 \quad (7)$$

Using Ohm's law, the equation for the relationship between phase A voltage magnitudes was expressed as in (8).

$$\boldsymbol{U_{A_m}} = \left(\boldsymbol{U_{A_n}} - \boldsymbol{I_{A_{mn}}} \mathrm{Z_S} - \boldsymbol{I_{B_{mn}}} \mathrm{Z_m} - \boldsymbol{I_{C_{mn}}} \mathrm{Z_m}\right) \quad (8)$$

To keep the variables in the optimization program independent of angle and to make equations linear, the square of equation (8) was used for optimization after some substitutions. Variables in non-convex terms ($U_A^R{}_n, I_A^R{}_{mn}, U_A^{Im}{}_n, I_A^{Im}{}_{mn}$) of square equation (8) were replaced by values obtained from load flow. The exact equation used is given in Appendix A as equation (A4).

2.2 Constraints

2.2.1 Voltage constraints

In Sri Lanka[30] statutory limit for voltage variation is ±6%. Therefore, the L-N voltage was maintained within ±6% of the nominal value. These limits were maintained as constants in the optimization algorithm.

$$216^2 \leq \left|\boldsymbol{U_{A_m}}\right|^2 \leq 244^2 \quad (9)$$

2.2.2 Inverter active power curtailment constraints

Capability to curtail entire active power generation is provided to inverters. However, the curtailment of active power was minimized using the objective function.

$$0 \leq P_{A_n}^{Cur} \leq \mathrm{P_{A_n}^G} \quad (10)$$

2.3 Cost functions

The minimization of the line losses and the inverter active power curtailment were considered to minimize the overall cost incurred for maintaining the voltage within the permissible range.

2.3.1 Cost of line losses

Line losses include the cost of Ohmic losses incurred in three-phase cables and neutral. Here, with the available variables, only the losses in three-phase lines were considered for the objective as:

$$\sum_{\forall i \in E}(\mathrm{R_{s_i}}) \times \left|\boldsymbol{I_{A_i}}\right|^2 + \sum_{\forall i \in E}(\mathrm{R_{s_i}}) \times \left|\boldsymbol{I_{B_i}}\right|^2 + \sum_{\forall i \in E}(\mathrm{R_{s_i}}) \times \left|\boldsymbol{I_{C_i}}\right|^2$$

With $L_{A,B,C_i} = \left|\boldsymbol{I_{A,B,C_i}}\right|^2$

$$\sum_{\forall i \in E}(\mathrm{R_{s_i}}) \times L_{A_i} + \sum_{\forall i \in E}(\mathrm{R_{s_i}}) \times L_{B_i} + \sum_{\forall i \in E}(\mathrm{R_{s_i}}) \times L_{C_i} \quad (11)$$

2.3.2 Cost of power curtailment

This term includes the power curtailment of every single-phase inverter, and it is expressed as in (12).

$$\sum_{\forall i \in N_A} P_A^{Cur}{}_i + \sum_{\forall i \in N_B} P_B^{Cur}{}_i + \sum_{\forall i \in N_C} P_C^{Cur}{}_i \quad (12)$$

2.4 Convex optimization problem

The nonlinear equality constraint in (7) is non-convex, and it is relaxed as in equation (13).

$$L_{A_{mn}} \geq \frac{p_{A_{mn}}^2}{W_{A_m}} + \frac{q_{A_{mn}}^2}{W_{A_m}} \quad (13)$$

Relaxed constraint (13) represents a second-order cone. Then additional linear inequality constraint as defined by equation (14) was used to add linear cuts to SOC relaxation from the second iteration onwards. Solutions are converged to a more optimum value in the first iteration, and the constants of equations in the second iteration were calculated from solutions generated in the first iteration. This upper bound was reduced in each iteration, gradually increasing the exactness of solutions. Squared current magnitude generated from a load flow using previous iteration's data was used as a part of the upper bound.

$$L_{A_{mn}} \leq \left|\boldsymbol{I_{A_{mn}\,(Load\ flow)}}\right|^2 + \frac{1000}{10^{iteration}} \quad (14)$$

Here, $\left|\boldsymbol{I}_{\boldsymbol{A_{mn}\,(Load\ flow)}}\right|^2$ is the squared magnitude of the current value generated from load flow from the previous iteration using OpenDSS. The term $\frac{1000}{10^{iteration}}$ in (14) is a constant for a particular iteration. It reduces to 100 in the third iteration. This constant was chosen empirically to gradually reduce search space. Additional search space from $\boldsymbol{I}_{\boldsymbol{A_{mn}\,(Load\ flow)}}$ was reduced ten times for subsequent iteration using $\frac{1000}{10^{iteration}}$ term. This acts as an increasingly tightening cutting planes to SOC relaxations in each phase. Because of this upper bound, sufficiently exact solutions that can be used to control the voltage of distribution networks were obtained after the third iteration of the optimization program. Equations (13) and (14) were repeated for the other two phases.

Then the optimization problem was represented by the sum of cost functions (11) and (12) as below subjected to the constraints given by (2), (3), (9), (10), (13), (14), A1, A2, and A4 for all 3 phases.

$$\text{minimize } \left\{\sum_{\forall i\in E}\left(\mathrm{R_{s_i}}\right)\times L_{A_i}+\sum_{\forall i\in E}\left(\mathrm{R_{s_i}}\right)\times L_{B_i}+\sum_{\forall i\in E}\left(\mathrm{R_{s_i}}\right)\times L_{C_i}\right\}+\left\{\sum_{\forall i\in N_A}{P_A^{Cur}}_i+\sum_{\forall i\in N_B}{P_B^{Cur}}_i+\sum_{\forall i\in N_C}{P_C^{Cur}}_i\right\} \quad (15)$$

2.5 Solution method

Three or fewer runs of the optimization program based on SOCP (equation (15)) were executed while reducing the upper bound of squared current (equation (14)). The optimization is performed for much larger convex terms with variables ($W_{A_m}, L_{A_{mn}}, p_{A_{mn}}, q_{A_{mn}}, Q_{A_n}^G, {P_A^{Cur}}_n$) while variables in non-convex terms ($U_{A\,n}^R, I_{A\,mn}^R, U_A^{Im}{}_n, I_A^{Im}{}_{mn}$) acting as constants for the considered iteration of the optimization program. When the number of iterations increases, updating terms become closer to the solution generated by solving the optimization problem. The flow chart of the algorithm is provided in Figure 2. First, a load flow was performed using OpenDSS with zero active power curtailment. Then the optimization problem implemented using CVX[31] was solved after updating $U_{A\,n}^R, I_{A\,mn}^R, U_A^{Im}{}_n, I_A^{Im}{}_{mn}$ terms in equations A1, A2, and A4 from the values obtained from the previous load flow. Then, P_A^{Cur}, P_B^{Cur}, and P_C^{Cur} were updated with the optimum curtailment values generated by solving the optimization problem. Next, a new load flow was performed with updated curtailment values. Then after updating equation (14) and $U_{A\,n}^R, I_{A\,mn}^R, U_A^{Im}{}_n, I_A^{Im}{}_{mn}$ terms in equations A1, A2, and A4 and using the values obtained from the last load flow, the optimization problem was solved. The repetition of 3 iterations of this process was sufficient to obtain

sufficiently exact solutions. This solution approach closely relates to the sequential convex programing.[32] Three iterations were chosen to reduce the cutting plane to 100 A from the square of load flow current in the final iteration. The first iteration is performed without a cutting plane. The second iteration is performed with the $\left|I_{A_{mn\ (Load\ flow)}}\right|^2$+1000 A cutting plane. Further increase of iterations increases the execution time without improving the exactness. Since the objective of this study is to obtain exact solutions faster, the proposed algorithm is designed to terminate with three iterations. Forward-backwards method based power flow iterations is used in load-flow to obtain required values for load currents that are used in the cutting plane.

This algorithm was implemented in Matlab with CVX optimization toolbox[31] and SDPT3 as the solver. OpenDSS was used to run the load flow and update variables in non-convex terms.

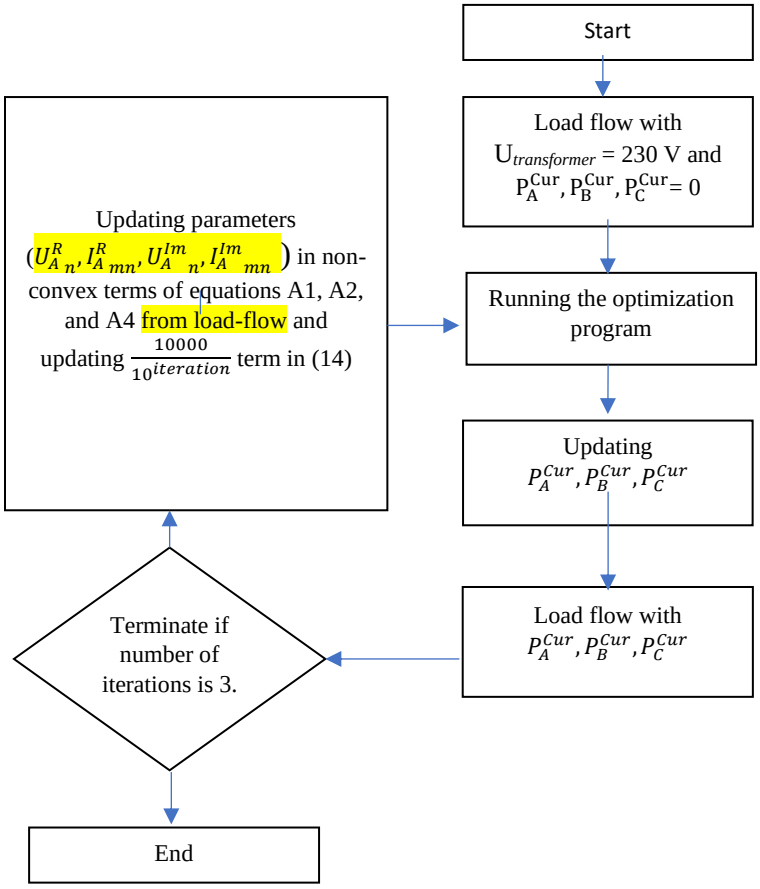

Figure 2 - Flow chart of the OPF solving algorithm

3. COMPARISON

The following optimization techniques are implemented and compared with the methodology suggested in this paper. The flow chart shown in Figure 3 was used for most of the methods described in subsequent sections.

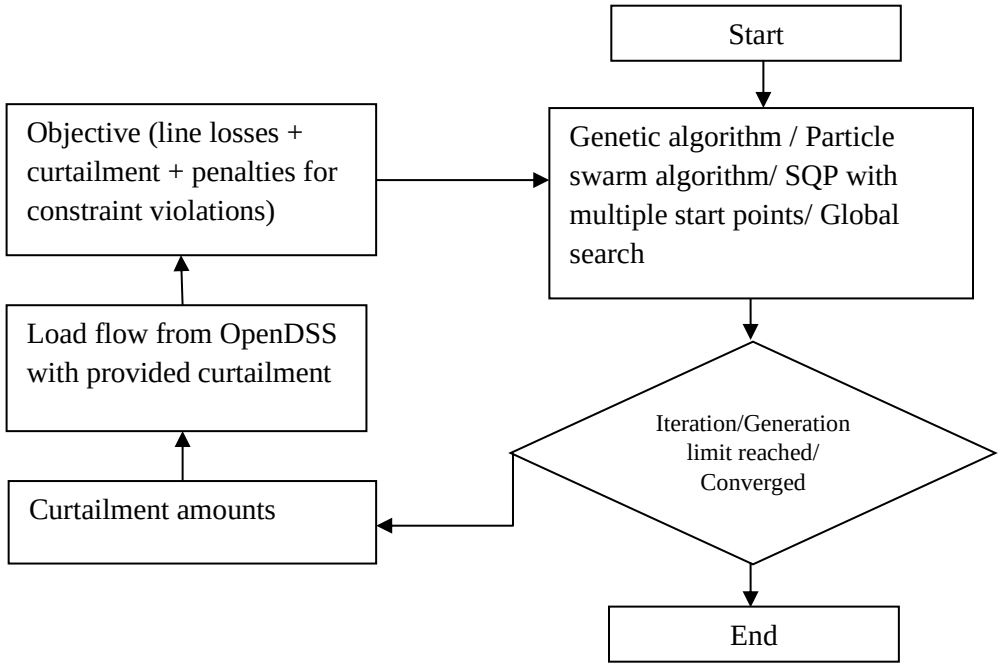

Figure 3 - Flow chart of other optimization algorithms

3.1 Linear programming-based technique

The methodology suggested by Robbins et al[10] was implemented and used for the comparison. In this method, the nonlinear terms in load flow equations have been replaced with first-order Taylor approximations, and it was assumed that voltage magnitudes of 3 phases of the same node are nearly similar. One load flow was performed using OpenDSS to provide operating points for linearization. The method was implemented using CVX in Matlab.

3.2 Semidefinite programming-based technique

The semidefinite programming-based method suggested by Gan et al[19] using branch flow model (BFM) was also implemented for comparison. The rank constraint was removed to make the problem convex. In this study, Gan's method was implemented using CVX in Matlab.

3.3 Sequence quadratic programming with multiple starting points

This method is used by Su et al[25] to solve the OPF in a low voltage four-wire distribution system. OpenDSS based load flow solving and penalty functions for voltage constraint violation were implemented as a black-box function. Matlab Multi-Start gradient-based solver was used to implement this algorithm. Uniformly distributed 20 start points were used.

3.4 Global Search

OpenDSS based load flow solving and penalty functions for voltage constraint violation were implemented as a black-box function. Matlab global search gradient-based solver was used to implement this algorithm. Unlike the multiple start point method, a scatter-search mechanism was used for generating start points.[33] Since gradient and hessian are not provided in both global search and SQP with multiple start points, and those are considerably slower than sequential SOCP and LP. However, the results of these two methods were used to compare the optimality of the proposed method.

3.5 Genetic Algorithm Optimization

Genetic algorithm-based OPFs were implemented using Matlab functions. Default values of Matlab built-in function were used for reproduction, mutation, cross-over, and migration options. Voltage constraints were added as penalty functions to the objective function. 30 generations were simulated for test case 1. 50 generations were simulated for test cases 2,3, and 4

3.6 Particle Swarm Optimization

Particle swarm optimization algorithm-based OPFs were implemented using Matlab functions. Default values of the Matlab built-in function were used. 30 iterations were simulated for test case 1. 50 iterations were simulated for test cases 2,3, and 4.

4. CASE STUDIES AND RESULTS

4.1 Test case 1

An underground European network given in[34] was selected as the second test case. The network diagram is presented in Figure 4. The network is a low voltage network with transposed lines. R/X ratio is higher than one in all line segments. Nodes with loads at phases A, B, and C are marked with red, green, and blue colours, respectively, and the load profile at 12 a.m. was selected. Randomly selected single-phase inverter capacities from 1 kVA to 7 kVA were placed in randomly selected 45 consumers from available 55 single-phase consumers. The PV generation profile (Figure 5) resulting in a voltage rise was selected for the case study. Irrespective of the vector group of the transformer, the angle of phase A of the low voltage side transformer bus is considered as zero. Angles of other phases were derived with reference to the angle of phase A voltage.

The details of the transformer are provided in **Table 1**.

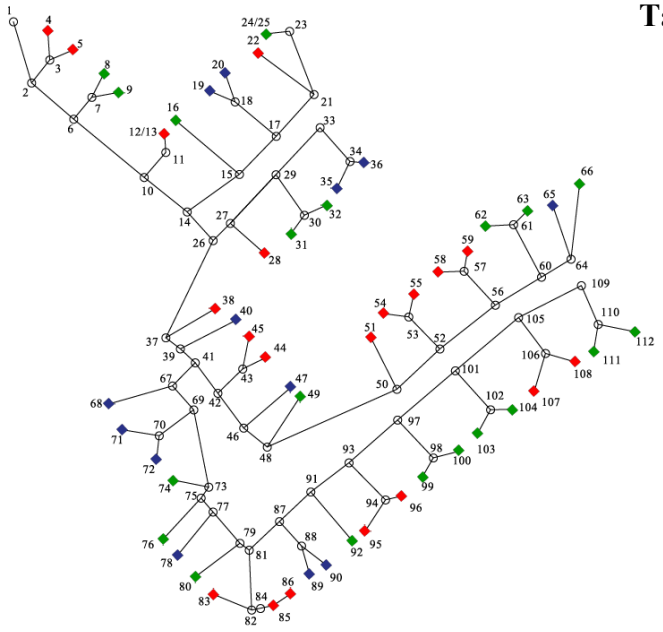

Figure 4 - Network diagram of test case 1

Table 1 - Details of transformer for test case 1

Primary voltage (L-L)	11 kV
Secondary voltage (L-L)	416 V
Capacity	0.8 MVA
Vector group	Δ/Y
Reactance (%)	4
Resistance (%)	0.4

For modelling the transformer, the reactance and resistance of the distribution transformer were added to the positive sequence reactance and resistance values of the first line section from bus 1 to 2. An ideal voltage source was connected to bus 1. Details of the cables provided in[34] were used for the simulation of two test cases. Simulations were performed in a PC with an Intel Core i7 @ 1.8 GHz processor and 8 GB RAM. Generation is 206.44 kW. The percentage of generation to load is 570%. Line loss without optimization is 9.15 kW.

A comparison of the simulation results of test case 1 is provided in **Table 2**. The comparison of voltage profiles of each simulation is provided in Appendix B.

The average voltage difference was calculated according to equation (16). This parameter is used as a measurement of the exactness of convex optimization-based methods.

$$\text{Average voltage difference (V)} = \frac{\sum|V_{optimization} - V_{load\ flow}|}{number\ of\ nodes} \quad (16)$$

Table 2 - Simulation results comparison (test case 1)

	Proposed method	Linear program (LP)	Genetic algorithm (GA)	Particle swarm (PS)
Execution time (s)	227.34	25.31	106,645.11	78,263.03
Objective (W) Line losses + curtailment	22,266.1	108,016	33879	27,969
Line losses (W)	6,251.1	1,816.0		
Curtailment (W)	16,015	106,200	27791	21,610.8
Average voltage difference (%)	0.0041	4.30	0	0

As shown in **Table 2**, the execution time of the proposed method is the second-lowest and next to the linear program (LP)-based method.[10] The value of the objective function is lesser in the proposed method compared to other accurate methods. The accuracy of the proposed method is significantly higher than the linear program-based method. As shown in Appendix B, voltage values of the linear programming-based method deviate from actual voltages by 14 V (6%) in some locations. This can lead to problems in voltage regulation. Therefore, the accuracy of the linear programming method is not sufficient for some practical applications. After 30 generations of GA and 30 iterations of PS, the proposed method is more optimum than GA and PS with acceptable average voltage difference for voltage control. The unique advantage of providing sufficiently exact solutions for voltage rise prevention in a shorter execution time using the proposed method is highlighted in this test case. Increase of accuracy with each iteration can be observed in Figure 6. SQP with multiple start points and global search algorithms were not

converged within 8 hours for this test case. For other methods, a comparison of phase C (phase with highest voltage rise) voltage profile is shown in Figure 7.

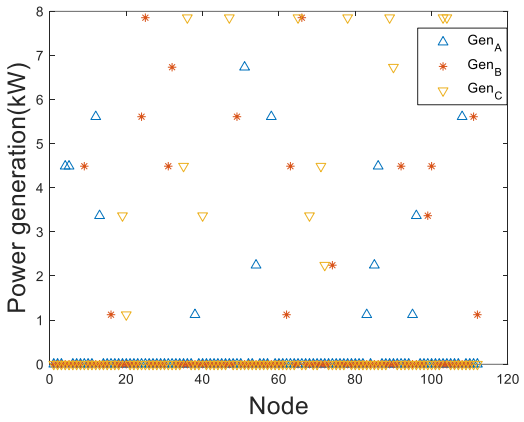

Figure 5 - PV generation data of test case 1

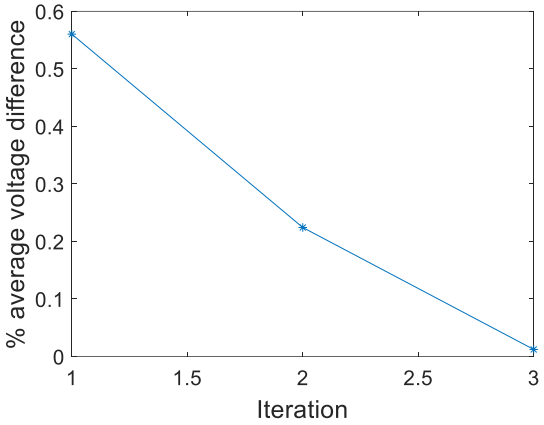

Figure 6 - %average voltage difference change with iterations – test case 1

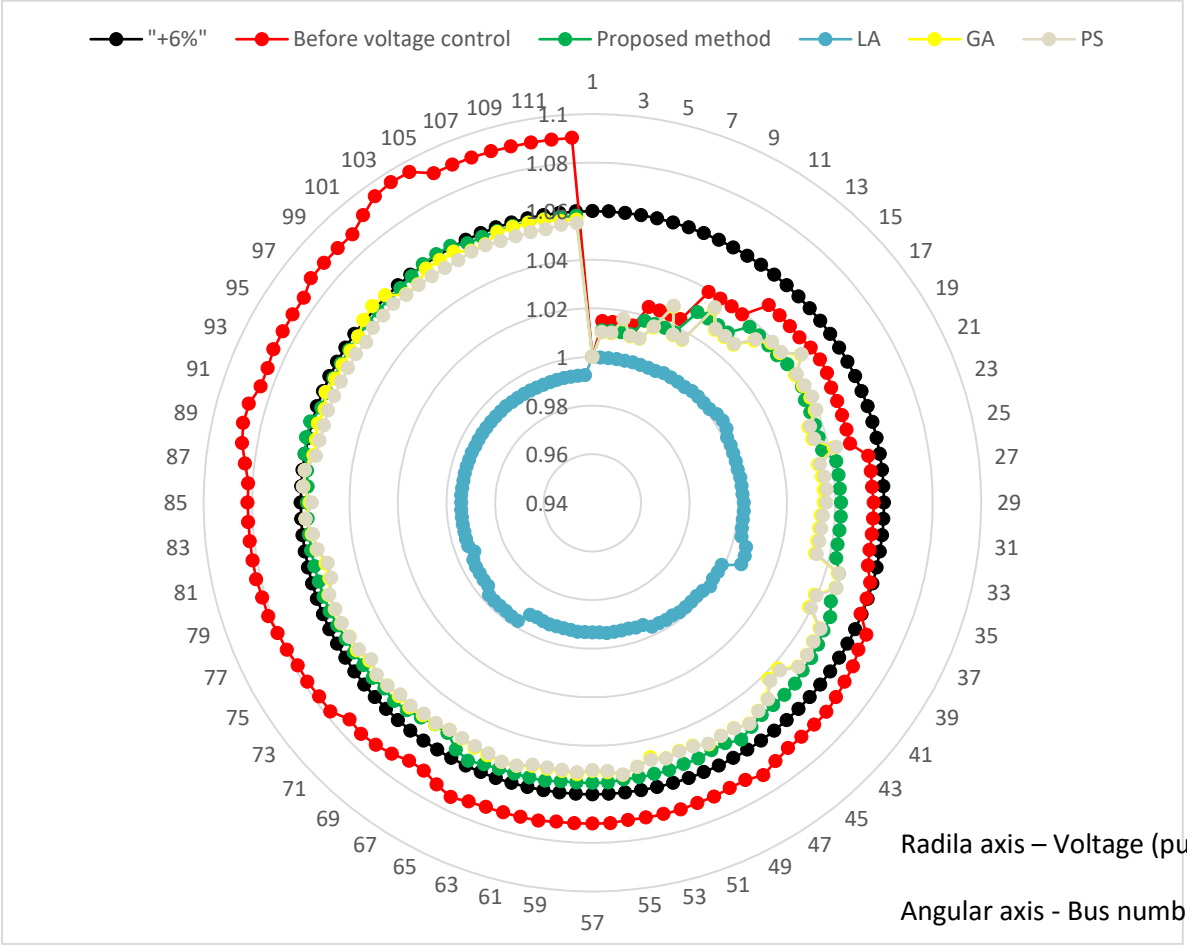

Figure 7 - Test case 1 phase C voltage comparison (pu)

4.4 Test case 2

IEEE 123 bus network is selected as the second case study. This network is a medium voltage (4.16 kV L-L) network with untransposed lines. R/X ratio is lower than one in most of the line segments. All the loads are considered as PQ loads. Loads of 4.16:0.48 kV transformer is added to the high voltage side and transformer is neglected in the simulation. The details of the transformer are provided in **Table 3**. Network diagram is provided in Figure 8.

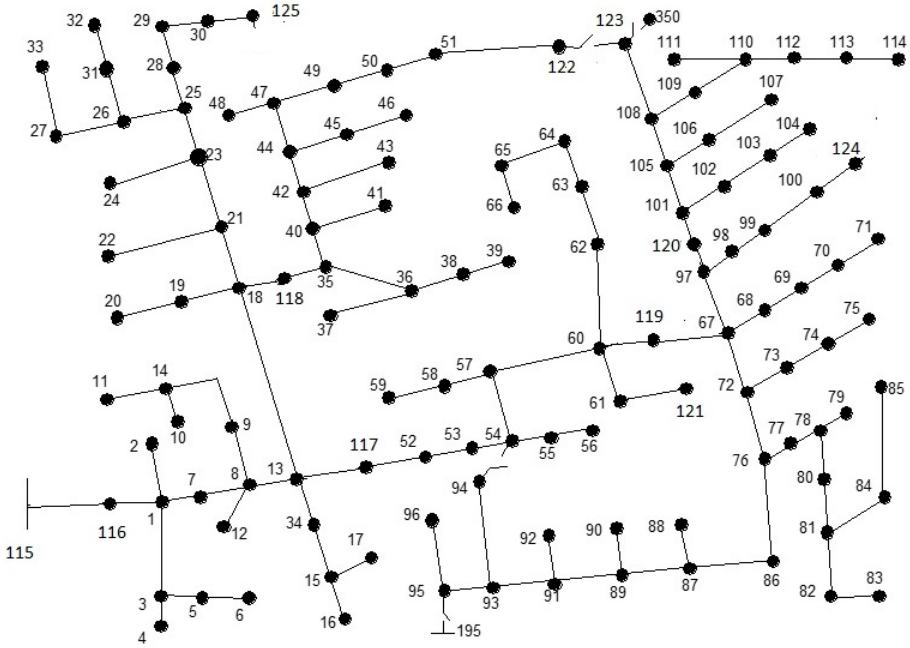

Figure 8 - Network diagram of test case 2

Table 3 – Details of the transformer for test case 2

Primary voltage (L-L)	115 kV
Secondary voltage (L-L)	4.16 kV
Capacity	5 MVA
Vector group	Δ/Y
Reactance (%)	8
Resistance (%)	1

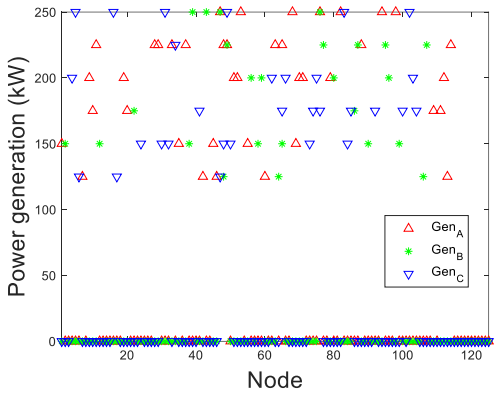

Figure 10 - PV generation data of test case 2

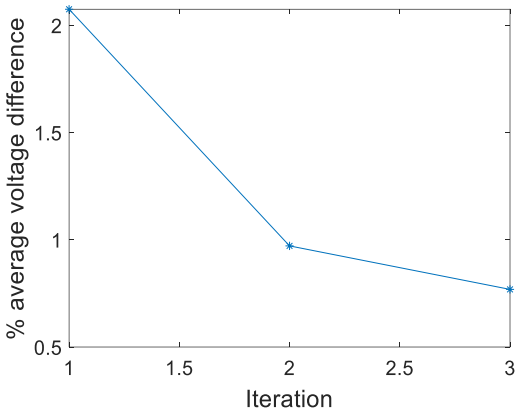

Figure 9 - %average voltage difference change with iterations – test case 2

Voltage regulators are neglected and voltage is kept within allowable range using distributed generators and active power curtailment. Generation is 18150 kW. The percentage of generation to load is 520%. Line loss without optimization is 1394.6kW.

Generation profile can be observed in Figure 10. Increase of accuracy with each iteration can be observed in Figure 9. As shown in Table 4, even though the execution time is lowest in LP, the average voltage difference is significantly higher than the proposed method. Voltage profile comparison for proposed method and LP against voltage profile of load-flow is provided in appendix B. The solutions provided by GA is more optimum than the proposed method while having a significantly higher execution time. SQP with multiple start points and global search algorithms were not converged within 8 hours for this test case. For other methods, a comparison of phase C (phase with highest voltage rise) voltage profile is shown in Figure 11.

Table 4 - Simulation results comparison (test case 2)

	Proposed method	Linear program (LP)	Genetic algorithm (Matlab built-in function)	Particle swarm (Matlab built-in function)
Execution time (s)	66.67	10.38	21167.17	13968.27
Objective (W) [Line losses + curtailment]	$1.75*10^6$	$1.45*10^6$	$1.51*10^6$	$1.90*10^6$
Line losses (W)	$1.3216*10^6$	$1.44617*10^6$	$1.37*10^6$	$1.3199*10^6$
Curtailment (W)	$4.2626*10^5$	0	$1.36*10^5$	$5.8397*10^5$
Average voltage difference (%)	0.8195	4.02	0	0

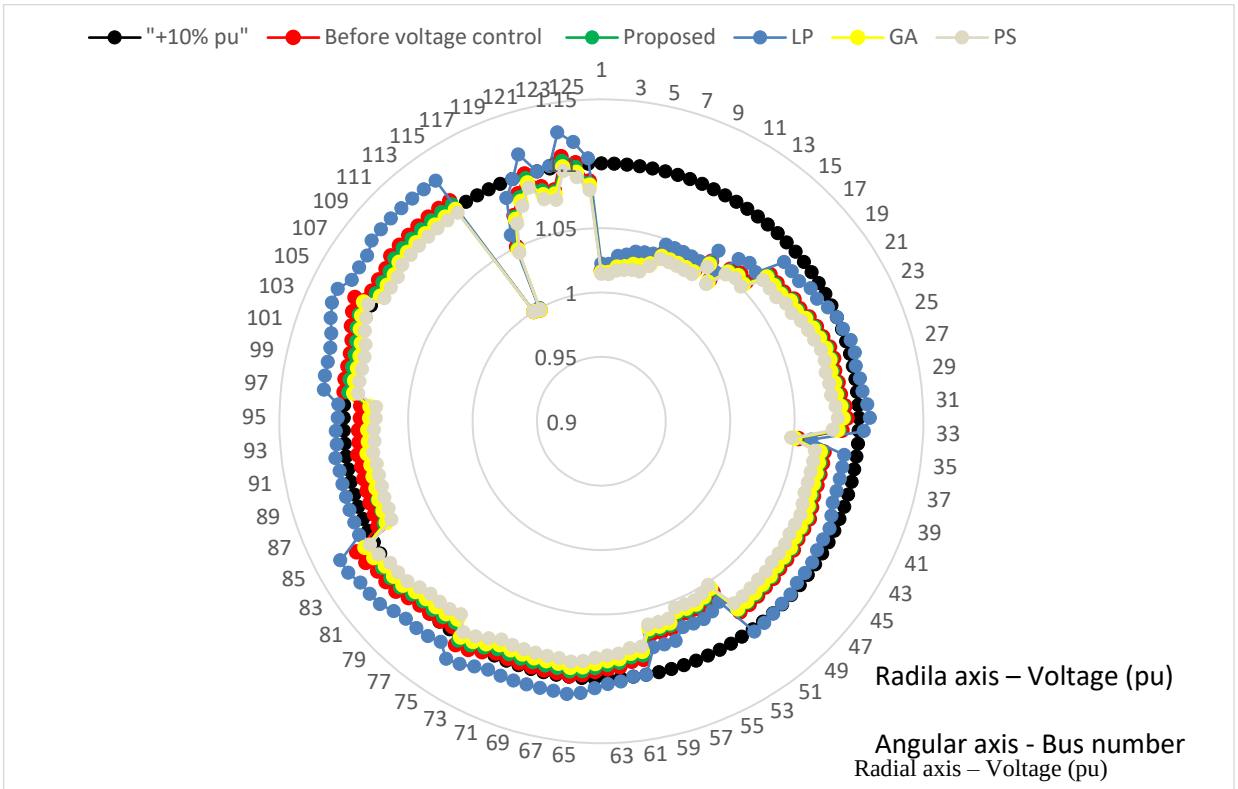

Figure 11 - Test case 3 phase C voltage compari

4.5 Test case 3

IEEE 33 bus network is selected as the fourth case study. This network is a balanced medium voltage (12.66 kV L-L) network with balanced three-phase loads. Test case 3 is used to analyze the performance of the optimization methods for balanced networks. R/X ratio is higher than one in all the line segments. All the loads are considered as PQ loads. Network diagram is shown in Figure 13. Generation is 16000kW. Four 4000 kW generators are placed as indicated in the network diagram. The percentage of generation to load is 430.68%. Line loss without optimization is 1670.8 kW.

Increase of accuracy with each iteration can be observed in Figure 12. Even though the execution time is lowest in LP, the average voltage difference is significantly higher than the proposed method. The solutions provided by GA, PS, SQP with multiple start points and Global search methods are more optimum than the proposed method while having significantly higher execution time. A comparison of phase C (phase with highest voltage rise) voltage profile of different optimization methods is shown in Figure 14.

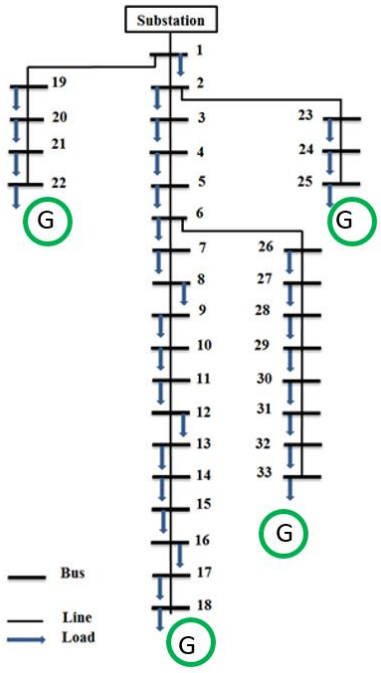

Figure 13 - Network diagram of test case 3

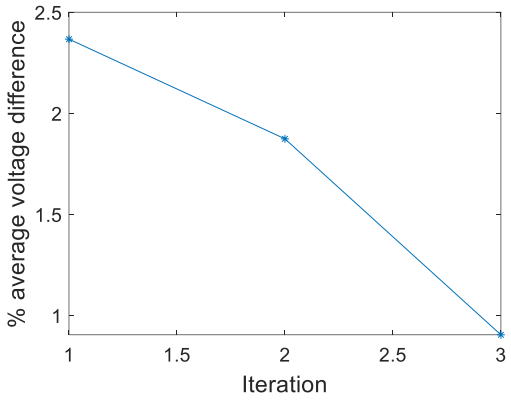

Figure 12 - %average voltage difference change with iterations – test case 3

Table 5 - Simulation results comparison (test case 3)

	Proposed method	Linear program	Genetic algorithm (Matlab built-in function)	Particle swarm (Matlab built-in function)	SQP with multiple start point (Matlab built-in function)	Global Search (Matlab built-in function)
Execution time (s)	20.09	4.02	586.49	695.94	1414.67	6279.24
Objective (W) [Line losses + curtailment]	$2.66*10^6$	$1.35*10^7$	$7.48*10^5$	$1.78*10^6$	$5.16*10^5$	$1.88*10^6$
Line losses (W)	$1.7341*10^6$	$1.0104*10^6$	$5.4859*10^5$	$1.0273*10^6$	$5.1333*10^5$	$9.5337*10^5$
Curtailment (W)	$9.2807*10^5$	$1.3492*10^7$	$1.9938*10^5$	$7.567*10^5$	$3.0211*10^3$	$926.52*10^3$
Average voltage difference (%)	0.90	670.70	0	0	0	0

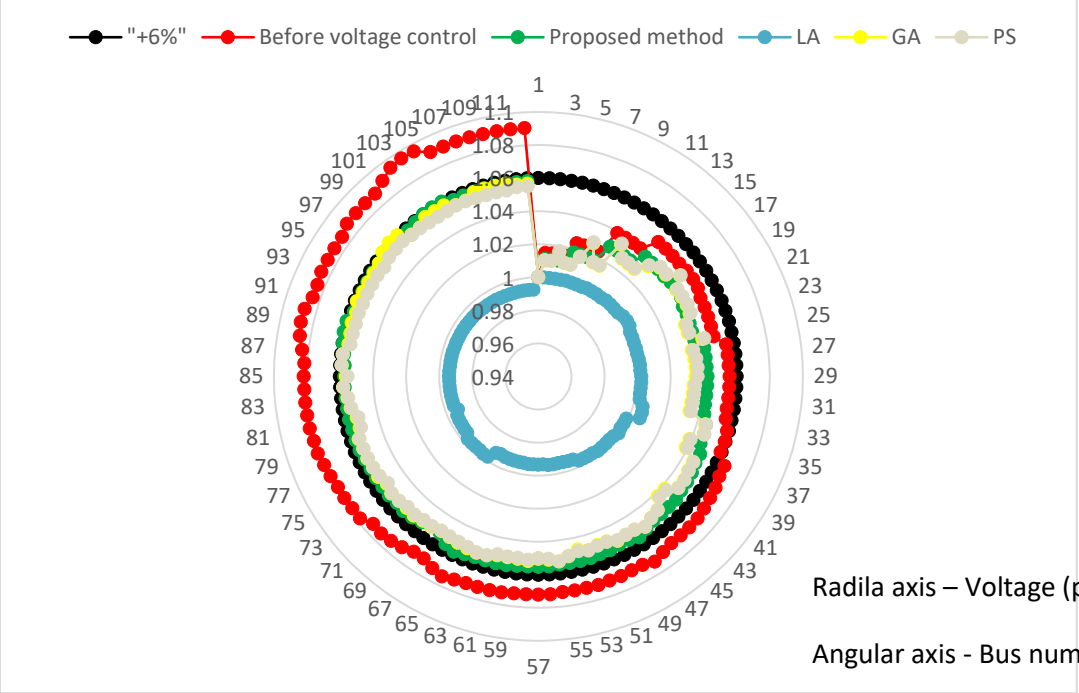

Figure 14 - Test case 4 phase C voltage comparison (pu)

5. CONCLUSION

The convex optimization-based OPF solving methods provide a faster execution time while compromising the exactness. To overcome this limitation, an optimum power flow algorithm based on the sequential second-order cone programming is proposed in this paper. The algorithm is utilized to maintain the voltage profile of unbalanced low and medium voltage distribution networks with distributed generators. Line losses and PV curtailments are used as the objective function with voltage and inverter active power curtailment constraints. A performance comparison was carried out in terms of optimality, exactness, and execution time for three test cases; test case 1 is an unbalanced LV network, test case 2 is an unbalanced MV network, and test case 3 is a balanced three-phase network.

The most optimum solution is provided by the proposed method for test case 1. It is 25% more optimum than the next best PS method while being 343% faster. For test case 2, the objective of the proposed method is within 15% of the most optimum solution provided by GA. However, the proposed method is 31 649% faster than the GA. For test case 3 most optimum solution is provided by the proposed method. It is 25% more optimum than the next best Global search while being $4.73 \_ 10^5$% faster. The proposed method is 343% to 31 649% faster than the best performing evolutionary computation techniques depending on the complexity of the test case. In terms of execution time, the proposed method is only second to the linear programming method while being $3.1 \_ 10^2$% to $1.05 \_ 10^5$% more accurate.

REFERENCES

1. Frank S, Steponavice I, Rebennack S. Optimal power flow: A bibliographic survey I Formulations and deterministic methods. *Energy Syst*. 2012;3(3):221-258. doi:10.1007/s12667-012-0056-y
2. Coffrin C, Hentenryck P Van. A Linear-Programming Approximation of AC Power Flows. *INFORMS J Comput*. Published online 2014:1-13. doi:10.1287/ijoc.2014.0594
3. Mahmoud K, Hussein MM, Abdel-Nasser M, Lehtonen M. Optimal Voltage Control in Distribution Systems with Intermittent PV Using Multiobjective Grey-Wolf-Lévy Optimizer. *IEEE Syst J*. 2020;14(1):760-770. doi:10.1109/JSYST.2019.2931829

4. Senjyu T, Miyazato Y, Yona A, Urasaki N, Funabashi T. Optimal distribution voltage control and coordination with distributed generation. *IEEE Trans Power Deliv*. 2008;23(2):1236-1242. doi:10.1109/TPWRD.2007.908816
5. Nguyen Q, Member S, Padullaparti H V, Member S, Lao K. Exact Optimal Power Dispatch in Unbalanced Distribution Systems with High PV Penetration. *IEEE Trans Power Syst*. 2018;8950(c):1-10. doi:10.1109/TPWRS.2018.2869195
6. Dall'Anese E, Giannakis GB, Wollenberg BF. Optimization of unbalanced power distribution networks via semidefinite relaxation. *2012 North Am Power Symp NAPS 2012*. Published online 2012. doi:10.1109/NAPS.2012.6336350
7. Nazir N, Racherla P, Almassalkhi M. Optimal Multi-Period Dispatch of Distributed Energy Resources in Unbalanced Distribution Feeders. *IEEE Trans Power Syst*. 2020;35(4):2683-2692. doi:10.1109/TPWRS.2019.2963249
8. Richardson P, Member S, Flynn D, Keane A. Optimal Charging of Electric Vehicles in Low-Voltage Distribution Systems. *IEEE Trans Power Syst*. 2012;27(1):268-279. doi:10.1109/TPWRS.2011.2158247
9. Yao E, Samadi P, Wong VWS, Schober R. Residential Demand Side Management Under High Penetration of Rooftop Photovoltaic Units. *IEEE Trans Smart Grid*. 2016;7(3):1597-1608. doi:10.1109/TSG.2015.2472523
10. Robbins BA, Domínguez-García AD. Optimal Reactive Power Dispatch for Voltage Regulation in Unbalanced Distribution Systems. *IEEE Trans Power Syst*. 2016;31(4):2903-2913. doi:10.1109/TPWRS.2015.2451519
11. Farivar M, Neal R, Clarke C, Low S. Optimal inverter VAR control in distribution systems with high PV penetration. *IEEE Power Energy Soc Gen Meet*. Published online 2012:1-7. doi:10.1109/PESGM.2012.6345736
12. Abdelouadoud SY, Girard R, Neirac FP, Guiot T. Optimal power flow of a distribution system based on increasingly tight cutting planes added to a second order cone relaxation. *Int J Electr Power Energy Syst*. 2015;69:9-17. doi:10.1016/j.ijepes.2014.12.084
13. Li Q, Vittal V. Convex Hull of the Quadratic Branch AC Power Flow Equations and Its Application in Radial Distribution Networks. *IEEE Trans Power Syst*. 2017;2016(1):1-9. doi:10.1109/TPWRS.2017.2712697
14. Low SH. Convex relaxation of optimal power flow-part II: Exactness. *IEEE Trans*

Control Netw Syst. 2014;1(2):177-189. doi:10.1109/TCNS.2014.2323634

15. Ji H, Wang C, Li P, et al. An enhanced SOCP-based method for feeder load balancing using the multi-terminal soft open point in active distribution networks. *Appl Energy*. 2017;208(August):986-995. doi:10.1016/j.apenergy.2017.09.051
16. Ranjan Jha R, Member S, Dubey A. Network-Level Optimization for Unbalanced Power Distribution System: Approximation and Relaxation.
17. Yuan Z, Hesamzadeh MR. Second-order cone AC optimal power flow: convex relaxations and feasible solutions. *J Mod Power Syst Clean Energy*. 2019;7(2):268-280. doi:10.1007/s40565-018-0456-7
18. Nazir N, Racherla P, Almassalkhi M. Optimal Multi-Period Dispatch of Distributed Energy Resources in Unbalanced Distribution Feeders. *IEEE Trans Power Syst*. 2020;35(4):2683-2692. doi:10.1109/TPWRS.2019.2963249
19. Gan L, Low SH. Convex relaxations and linear approximation for optimal power flow in multiphase radial networks. *Proc - 2014 Power Syst Comput Conf PSCC 2014*. Published online 2014. doi:10.1109/PSCC.2014.7038399
20. Louca R, Seiler P, Bitar E. A rank minimization algorithm to enhance semidefinite relaxations of Optimal Power Flow. *2013 51st Annu Allert Conf Commun Control Comput Allert 2013*. Published online 2013:1010-1020. doi:10.1109/Allerton.2013.6736636
21. Lesieutre BC, Molzahn DK, Borden AR, DeMarco CL. Examining the limits of the application of semidefinite programming to power flow problems. *2011 49th Annu Allert Conf Commun Control Comput Allert 2011*. Published online 2011:1492-1499. doi:10.1109/Allerton.2011.6120344
22. Somayeh Sojoudi* RM and JL. Low-Rank Solution of Convex Relaxation for Optimal Power Flow Problem. In: *IEEE SmartGridComm 2013 Symposium - Support for Storage, Renewable Resources and Micro-Grids*. ; 2013:636-641.
23. Hijazi H, Coffrin C, Hentenryck P Van. Convex quadratic relaxations for mixed-integer nonlinear programs in power systems. *Math Program Comput*. 2017;9(3):321-367. doi:10.1007/s12532-016-0112-z
24. Gan L, Li N, Topcu U, Low SH. Exact Convex Relaxation of Optimal Power Flow in Radial Networks. *IEEE Trans Automat Contr*. 2015;60(1):72-87. doi:10.1109/TAC.2014.2332712

25. Su X, Masoum MAS, Wolfs PJ. Optimal PV Inverter Reactive Power Control and Real Power Curtailment to Improve the Performance of Low Voltage Distribution System. *IEEE Trans Sustain Energy*. 2014;5(3):967-977.
26. Gopalakrishnan A, Raghunathan AU, Nikovski D, Biegler LT. Global optimization of Optimal Power Flow using a branch & bound algorithm. *2012 50th Annu Allert Conf Commun Control Comput Allert 2012*. Published online 2012:609-616. doi:10.1109/Allerton.2012.6483274
27. Boyd S, Mattingley J. Branch and Bound Methods. Published online 2018:1-18.
28. Kersting WH. *Distribution System Modelling and Analysis*. CRC Press; 2002.
29. Baran ME, Wu FF. Optimal sizing of capacitors placed on a radial distribution system. *IEEE Trans Power Deliv*. 1989;4(1):735-743. doi:10.1109/61.19266
30. Public Utilities Commission SL. *DISTRIBUTION CODE OF SRI LANKA*.; 2012. https://www.ceb.lk/front_img/img_reports/1532500020Distribution_Code.pdf
31. M. Grant, S. Boyd and YY. CVX: Matlab Software for Disciplined Convex Programming. http://www.stanford.edu/~boyd/cvx
32. Schittkowski K, Zillober C. Sequential Convex Programming Methods. Published online 1995:123-141. doi:10.1007/978-3-642-88272-2_8
33. Matlab. How GlobalSearch and MultiStart Work. https://in.mathworks.com/help/gads/how-globalsearch-and-multistart-work.html
34. Soceity IP and energy. European Low Voltage Test Feeder. IEEE Power and energy Soceity. Published 2015. Accessed February 14, 2020. https://site.ieee.org/pes-testfeeders/resources/

APPENDIX A

The equations (A1) and (A2) were obtained by expanding equations (2) and (3). Variables in non-convex terms ($U_A^R{}_n, I_A^R{}_{mn}, U_A^{Im}{}_n, I_A^{Im}{}_{mn}$) were replaced from respective values obtained from the load flow. Then, $W_{A_m} = |\boldsymbol{U_{A_m}}|^2$ and $L_{A_{mn}} = |\boldsymbol{I_{A_{mn}}}|^2$ substitutions were made to make the equations linear.

$$p_{A_{mn}} = \sum_{k:(j,k)\in E} p_{A_{nk}} + \mathrm{P}^{\mathrm{C}}_{\mathrm{A_n}} - \mathrm{P}^{\mathrm{G}}_{\mathrm{A_n}} + \mathrm{R}_{\mathrm{s_{mn}}} L_{A_{mn}} + \mathrm{R}_{\mathrm{m_{mn}}}\left(I^R_{A\,mn}\, I^R_{B\,mn} + I^{Im}_{A\,mn}\, I^{Im}_{B\,mn}\right) - \mathrm{X}_{\mathrm{m_{mn}}}\left(I^R_{A\,mn}\, I^{Im}_{B\,mn} - I^{Im}_{A\,m}\, I^R_{B\,m}\right) + \mathrm{R}_{\mathrm{m_{mn}}}\left(I^R_{A\,mn}\, I^R_{C\,mn} + I^{Im}_{A\,mn}\, I^{Im}_{C\,mn}\right) - \mathrm{X}_{\mathrm{m_{mn}}}\left(I^R_{A\,mn}\, I^{Im}_{C\,mn} - I^{Im}_{A\,m}\, I^R_{C\,m}\right) \quad \text{(A1)}$$

$$q_{A_{mn}} = \sum_{k:(j,k)\in E} q_{A_{nk}} + \mathrm{Q}^{\mathrm{C}}_{\mathrm{A_n}} + Q^G_{A_n} + \mathrm{X}_{\mathrm{s_{mn}}} L_{A_{mn}} + \mathrm{X}_{\mathrm{m_{mn}}}\left(I^R_{A\,mn}\, I^R_{B\,mn} + I^{Im}_{A\,mn}\, I^{Im}_{B\,mn}\right) + \mathrm{R}_{\mathrm{m_{mn}}}\left(I^R_{A\,mn}\, I^{Im}_{B\,mn} - I^{Im}_{A\,m}\, I^R_{B\,m}\right) + \mathrm{X}_{\mathrm{m_{mn}}}\left(I^R_{A\,mn}\, I^R_{C\,mn} + I^{Im}_{A\,mn}\, I^{Im}_{C\,mn}\right) + \mathrm{R}_{\mathrm{m_{mn}}}\left(I^R_{A\,mn}\, I^{Im}_{C\,mn} - I^{Im}_{A\,m}\, I^R_{C\,m}\right) \quad \text{(A2)}$$

Derivation of equation A4:

$$\mathbf{U_{A_m}} = \left(\mathbf{U_{A_n}} - \mathbf{I_{A_{mn}} Z_S} - \mathbf{I_{B_{mn}} Z_m} - \mathbf{I_{C_{mn}} Z_m}\right) \quad (8)$$

After separating real and imaginary parts equation (8) was expressed as follows.

$$\mathbf{U_{A_m}} = U^R_{A_n} + U^{Im}_{A\,n} j - \left(I^R_{A_{mn}} + jI^{Im}_{A\,mn}\right)\left(R_{S_{mn}} + jX_{S_{mn}}\right) - \left(I^R_{B_{mn}} + jI^{Im}_{B\,mn}\right)\left(R_{m_{mn}} + jX_{m_{mn}}\right) - \left(I^R_{C_{mn}} + jI^{Im}_{C\,mn}\right)\left(R_{m_{mn}} + jX_{m_{mn}}\right)$$

After multiplications between current and resistance terms following equation was obtained.

$$U^R_{A\,m} + U^{Im}_{A\,m} j = U^R_{A\,n} + jU^{Im}_{A\,n} - \left\{R_{S_{mn}} I^R_{A\,mn} + jX_{S_{mn}} I^R_{A\,mn} + jR_{S_{mn}} I^{Im}_{A\,mn} - X_{S_{mn}} I^{Im}_{A\,mn}\right\} - \left\{R_{m_{mn}} I^R_{B\,mn} + jX_{m_{mn}} I^R_{B\,mn} + jR_{m_{mn}} I^{Im}_{B\,mn} - X_{m_{mn}} I^{Im}_{B\,mn}\right\} - \left\{R_{m_{mn}} I^R_{C\,mn} + jX_{m_{mn}} I^R_{C\,mn} + jR_{m_{mn}} I^{Im}_{C\,mn} - X_{m_{mn}} I^{Im}_{C\,mn}\right\}$$

Squared magnitude of complex number is obtained after summation of squares of real and imaginary parts.

$$\left|\boldsymbol{U_{A_m}}\right|^2 = \left(U^R_{A\,n} - R_{S_{mn}} I^R_{A\,mn} + X_{S_{mn}} I^{Im}_{A\,mn} - R_{m_{mn}} I^R_{B\,mn} + X_{m_{mn}} I^{Im}_{B\,mn} - R_{m_{mn}} I^R_{C\,mn} + X_{m_{mn}} I^{Im}_{C\,mn}\right)^2 + \left(U^{Im}_{A\,n} - X_{S_{mn}} I^R_{A\,mn} - R_{S_{mn}} I^{Im}_{A\,mn} - X_{m_{mn}} I^R_{B\,mn} - R_{m_{mn}} I^{Im}_{B\,mn} - X_{m_{mn}} I^R_{C\,mn} - R_{m_{mn}} I^{Im}_{C\,mn}\right)^2 \quad \text{(A3)}$$

After expanding above A3, simplification and substituting from equation (7), equation A4 was obtained.

$$W_{A_m} = W_{A_n} + \mathrm{R_{S_{mn}}}^2 L_{A_{mn}} + \mathrm{X_{S_{mn}}}^2 L_{A_{mn}} + \mathrm{R_{m_{mn}}}^2 L_{B_{mn}} + \mathrm{X_{m_{mn}}}^2 L_{B_{mn}} + \mathrm{R_{m_{mn}}}^2 L_{C_{mn}} +$$
$$\mathrm{X_{m_{mn}}}^2 L_{C_{mn}} - 2\, p_{mn_A} - 2\, q_{mn_A} - 2V_A^R{}_n \mathrm{R_{m_{mn}}} I_B^R{}_{mn} + 2V_A^R{}_n \mathrm{X_{m_{mn}}} I_B^{Im}{}_{mn} -$$
$$2V_A^R{}_n \mathrm{R_{m_{mn}}} I_C^R{}_{mn} + 2V_A^R{}_n \mathrm{X_{m_{mn}}} I_C^{Im}{}_{mn} - 2V_A^{Im}{}_n \mathrm{X_{m_{mn}}} I_B^R{}_{mn} - 2V_A^{Im}{}_n \mathrm{R_{m_{mn}}} I_B^{Im}{}_{mn} -$$
$$2V_A^{Im}{}_n \mathrm{X_{m_{mn}}} I_C^R{}_{mn} - 2V_A^{Im}{}_n \mathrm{R_{m_{mn}}} I_C^{Im}{}_{mn} + 2\mathrm{R_{S_{mn}}} I_A^R{}_{mn} \mathrm{R_{m_{mn}}} I_B^R{}_{mn} -$$
$$2\mathrm{R_{S_{mn}}} I_A^R{}_{mn} \mathrm{X_{m_{mn}}} I_B^{Im}{}_{mn} + 2\mathrm{R_{S_{mn}}} I_A^R{}_{mn} \mathrm{R_{m_{mn}}} I_C^R{}_{mn} - 2\mathrm{R_{S_{mn}}} I_A^R{}_{mn} \mathrm{X_{m_{mn}}} I_C^{Im}{}_{mn} -$$
$$2\mathrm{X_{S_{mn}}} I_A^{Im}{}_{mn} \mathrm{R_{m_{mn}}} I_B^R{}_{mn} + 2\mathrm{X_{S_{mn}}} I_A^{Im}{}_{mn} \mathrm{X_{m_{mn}}} I_B^{Im}{}_{mn} - 2\mathrm{X_{S_{mn}}} I_A^{Im}{}_{mn} \mathrm{R_{m_{mn}}} I_C^R{}_{mn} -$$
$$2\mathrm{X_{S_{mn}}} I_A^{Im}{}_{mn} \mathrm{X_{m_{mn}}} I_C^{Im}{}_{mn} + 2\mathrm{R_{m_{mn}}} I_B^R{}_{mn} \mathrm{R_{m_{mn}}} I_C^R{}_{mn} - 2\mathrm{R_{m_{mn}}} I_B^R{}_{mn} \mathrm{X_{m_{mn}}} I_C^{Im}{}_{mn} +$$
$$2\mathrm{X_{m_{mn}}} I_B^{Im}{}_{mn} \mathrm{X_{m_{mn}}} I_C^{Im}{}_{mn} + 2\mathrm{X_{S_{mn}}} I_A^R{}_{mn} \mathrm{X_{m_{mn}}} I_B^R{}_{mn} + 2\mathrm{X_{S_{mn}}} I_A^R{}_{mn} \mathrm{R_{m_{mn}}} I_B^{Im}{}_{mn} +$$
$$2\mathrm{X_{S_{mn}}} I_A^R{}_{mn} \mathrm{X_{m_{mn}}} I_C^R{}_{mn} + 2\mathrm{X_{S_{mn}}} I_A^R{}_{mn} \mathrm{R_{m_{mn}}} I_C^{Im}{}_{mn} + 2\mathrm{R_{S_{mn}}} I_A^{Im}{}_{mn} \mathrm{X_{m_{mn}}} I_B^R{}_{mn} +$$
$$2\mathrm{R_{S_{mn}}} I_A^{Im}{}_{mn} \mathrm{R_{m_{mn}}} I_B^{Im}{}_{mn} + 2I_A^{Im}{}_{mn} \mathrm{X_{m_{mn}}} I_C^R{}_{mn} + 2\mathrm{R_{S_{mn}}} I_A^{Im}{}_{mn} \mathrm{R_{m_{mn}}} I_C^{Im}{}_{mn} +$$
$$2\mathrm{X_{m_{mn}}} I_B^R{}_{mn} \mathrm{X_{m_{mn}}} I_C^R{}_{mn} + 2\mathrm{X_{m_{mn}}} I_B^R{}_{mn} \mathrm{R_{m_{mn}}} I_C^{Im}{}_{mn} + 2\mathrm{R_{m_{mn}}} I_B^{Im}{}_{mn} \mathrm{R_{m_{mn}}} I_C^{Im}{}_{mn} \qquad \text{(A4)}$$

APPENDIX B

Figure B1 and B2 shows the voltage profile of the linear programming and the proposed method for test case 1. The voltage difference between linear program and load flow executed using curtailment values obtained from the linear program is highlighted using curly brackets in figure B2. Voltage differences around 14 V were observed in some nodes. These types of deviations can generate voltage variations above or below the permissible ±6% voltage margin. Compared to the linear program, average voltage deviations are lower by $1.048*10^5$% in the proposed method. V_A, V_B, V_C are voltage values generated from the optimization program (linear program or proposed

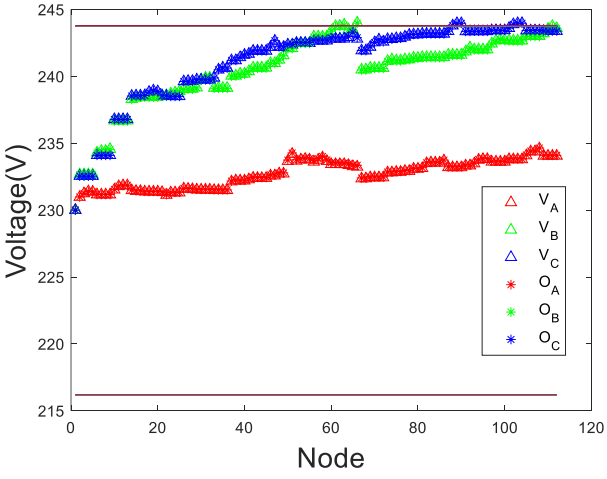

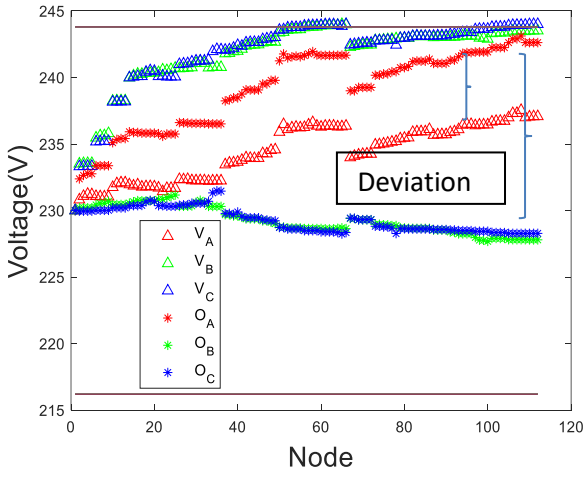

method) when determining optimum curtailment. O_A, O_B, O_C are voltage values generated from the load flow executed using curtailment values generated from the optimization program.

Figure B3 and B4 shows the voltage profile of the proposed method and the linear programming for test case 3. The voltage difference between linear program and load flow executed using curtailment values obtained from the linear program is highlighted using curly brackets in figure B4. Voltage differences around 200 V were observed in some nodes. These types of deviations can generate voltage variations above or below the permissible ±10% voltage margin. Compared to the linear program, average voltage deviations are lower by $7.45*10^4$% in the proposed method.

Figure B1 – Voltage profile test case 1 (Proposed

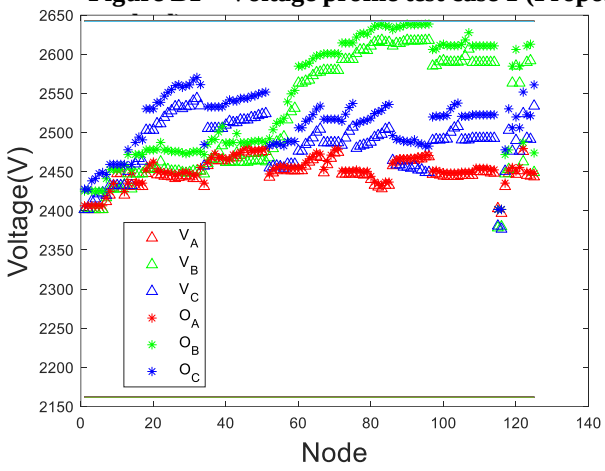

Figure B3 - Figure B3 - Voltage profile test case 2 (Proposed method)

Figure B2 – Voltage profile test case 1 (Linear

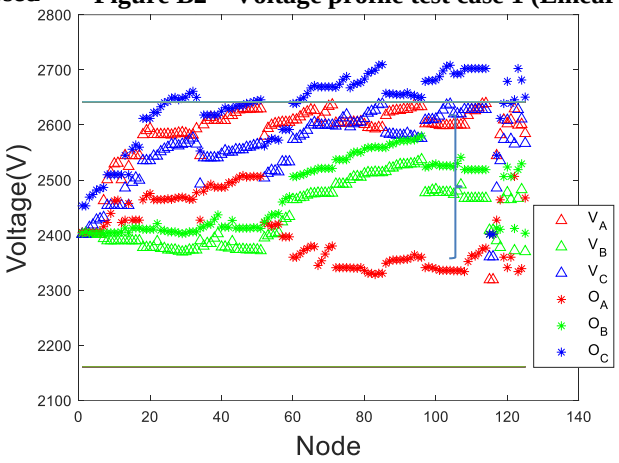

Figure B4 - Voltage profile test case 2 (Linear Program)